

1 **Early beta oscillations in multisensory association** 2 **areas underlie crossmodal performance enhancement**

3 Georgios Michail, Daniel Senkowski, Martin Holtkamp, Bettina Wächter, Julian Keil

4

5 **Abstract**

6 The combination of signals from different sensory modalities can enhance perception
7 and facilitate behavioral responses. While previous research described crossmodal
8 influences in a wide range of tasks, it remains unclear how such influences drive
9 performance enhancements. In particular, the neural mechanisms underlying
10 performance-relevant crossmodal influences, as well as the latency and spatial profile
11 of such influences are not well understood. Here, we examined data from high-density
12 electroencephalography (N = 30) and electrocorticography (N = 4) recordings to
13 characterize the oscillatory signatures of crossmodal facilitation of response speed, as
14 manifested in the speeding of visual responses by concurrent task-irrelevant auditory
15 information. Using a data-driven analysis approach, we found that individual gains in
16 response speed correlated with reduced beta power (13-25 Hz) in the audiovisual
17 compared with the visual condition, starting within 80 ms after stimulus onset in
18 multisensory association and secondary visual areas. In addition, the
19 electrocorticography data revealed a beta power suppression in audiovisual compared
20 with visual trials in the superior temporal gyrus (STG). Our data suggest that the
21 crossmodal facilitation of response speed is associated with early beta power in
22 multisensory association and secondary visual areas, presumably reflecting the
23 enhancement of early sensory processing through selective attention. This finding
24 furthers our understanding of the neural correlates underlying crossmodal response

25 speed facilitation and highlights the critical role of beta oscillations in mediating
26 behaviorally relevant audiovisual processing.

27

28 **Significance Statement**

29 The use of complementary information across multiple senses can enhance perception.
30 Previous research established a central role of neuronal oscillations in multisensory
31 perception, but it remains poorly understood how they relate to multisensory
32 performance enhancement. To address this question, we recorded electrophysiological
33 signals from scalp and intracranial electrodes (implanted for presurgical monitoring) in
34 response to simple visual and audiovisual stimuli. We then associated the difference in
35 oscillatory power between the two conditions with the speeding of responses in the
36 audiovisual trials. We demonstrate, that the crossmodal facilitation of response speed
37 is associated with beta power in multisensory association areas during early stages of
38 sensory processing. This finding highlights the importance of beta oscillations in
39 mediating behaviorally relevant audiovisual processing.

40

41 **Introduction**

42

43 In everyday life, using complementary information from multiple sensory modalities is
44 often critical to make rapid and accurate perceptual decisions. The synthesis of signals
45 from different senses has been shown to improve perceptual performance, leading to
46 more accurate (Spence and Driver, 2004; Lippert et al., 2007) and faster responses
47 (Hershenson, 1962; Diederich and Colonius, 2004). Previous research has shown that
48 crossmodal interactions are governed by neural oscillations in different frequency bands
49 that can occur at both early and late stages of processing and involve bottom-up and
50 top-down mechanisms (Keil and Senkowski, 2018; Bauer et al., 2020). Despite the

51 considerable progress in characterizing the role of neural oscillations in multisensory
52 processing, it remains unclear how they relate to the behavioral facilitation of responses
53 to multisensory stimuli. In particular, the processing stage at which functionally relevant
54 oscillations unfold during crossmodal behavior facilitation, and whether they reflect top-
55 down or bottom-up influences on sensory processing, are key questions that are not
56 well understood (Bizley et al., 2016).

57
58 In relation to the crossmodal facilitation of response times (RTs), electrophysiological
59 studies in humans examining multisensory interactions in evoked brain potentials have
60 suggested a link of RT facilitation with early crossmodal interactions (Giard and
61 Peronnet, 1999; Fort et al., 2002; Molholm et al., 2004; Gondan et al., 2005). However,
62 the proposed association in these studies is based on activity differences between
63 multisensory and unisensory conditions that were not directly linked with the individual
64 gains in multisensory performance enhancement. Thus far, only few studies have
65 examined how neural oscillations relate to crossmodal RT facilitation across individuals
66 (Senkowski et al., 2006; Mercier et al., 2015). In a speeded response paradigm,
67 Senkowski et al. (2006) found a relationship between evoked beta oscillations and
68 shorter RTs for unisensory and bisensory audiovisual stimuli. In an electrocorticography
69 (ECoG) study, Mercier et al. (2015) observed that delta band (<4 Hz) phase alignment
70 in a sensorimotor network was related to crossmodal facilitation of response speed.
71 However, in both studies the modulations in neural oscillations were associated with
72 shorter RTs after both multisensory and unisensory stimulation. Therefore, it cannot be
73 concluded that these brain responses are specific for crossmodal facilitation of RTs.
74 Moreover, the use of speeded responses in these studies, with a mean RT lower than
75 300 ms for audiovisual trials, indicates that the observed oscillatory activities may reflect
76 motor-related processing. Taken together, while there is some evidence that neural

77 oscillations play a role in crossmodal facilitation of response speed, the specificity of
78 these effects to multisensory processing has not yet been demonstrated. Critically, it
79 remains unclear whether the crossmodal facilitation of response speed is associated
80 with modulations of neural oscillations during early stages of sensory processing.

81
82 In two experiments, we examined how individual gains in response speed during
83 crossmodal stimulation relate to neural processing, as reflected in neural oscillations.
84 We investigated oscillatory power in response to unisensory visual and bisensory
85 audiovisual stimuli in experiments in which participants had to indicate the number of
86 perceived flashes. Electrophysiological data were collected independently in healthy
87 individuals (N = 30) using high-density EEG recordings and in patients with drug-
88 resistant focal epilepsy (N = 4) prior to resective surgery, using ECoG recordings. The
89 EEG data analysis revealed that lower early beta band power for audiovisual compared
90 with visual trials in multisensory association and secondary visual regions correlated
91 with crossmodal facilitation in response speed. The ECoG data analysis revealed lower
92 beta power in audiovisual compared with visual trials in the superior temporal gyrus
93 (STG). Our findings suggest that early beta band power in multisensory association
94 cortex plays an important role in crossmodal facilitation of response speed.

95

96 **Material and Methods**

97 The electrophysiological data from high-density scalp EEG and intracranial ECoG
98 recordings were obtained independently. Throughout the text, the recording sessions to
99 obtain these data are referred to as 'EEG experiment' and 'ECoG experiment',
100 respectively.

101

102 **Participants**

103 For the EEG experiment, forty participants (mean age \pm standard deviation (SD): 26.6
104 \pm 7.8 years; 19 females) with normal hearing, normal or corrected-to-normal vision and
105 no history of neurological disorders were recruited. Six participants with excessive EEG
106 artefacts (slow wave drifts and muscular artefacts) and four with insufficient trials (less
107 than 30 trials in at least one of the analyzed conditions) were excluded from the analysis.
108 Therefore, a subset of thirty participants (mean age \pm SD: 25.5 \pm 6.4 years; 17 females)
109 was included in further EEG data analyses.

110
111 Four male patients (mean age \pm SD: 27.3 \pm 4.9 years) with drug-resistant focal epilepsy
112 treated at the Epilepsy-Center Berlin-Brandenburg (Institute for Diagnostic of Epilepsy)
113 in Berlin participated in the ECoG experiment. The patients were implanted with
114 subdural electrodes (n = 66, 50, 40 and 74 for patients 1 to 4, respectively) covering
115 mainly the temporal cortex for presurgical intracranial video-EEG monitoring.

116
117 All participants provided written informed consent. The experiments were conducted in
118 accordance with the 2008 Declaration of Helsinki and approved by the ethics committee
119 of the Charité–Universitätsmedizin Berlin (Approval number: EA1/207/15).

120

121 **Experimental Design**

122 Participants were presented with combinations of auditory and visual stimuli and had to
123 indicate the number of perceived visual stimuli. Stimulus combinations consisted of 0, 1
124 or 2 auditory (a) stimuli combined with either 0, 1 or 2 visual (v) stimuli. Six stimulus
125 combinations were used in the EEG experiment, (a₀v₁, a₀v₂, a₁v₁, a₂v₀, a₂v₁, a₂v₂), and
126 nine in the ECoG experiment (a₀v₁, a₀v₂, a₁v₀, a₁v₁, a₁v₂, a₂v₀, a₂v₁, a₂v₂ and a₂v₁late).
127 The current study focused on the analysis of the visual-only stimulus (a₀v₁, **V**) and the
128 bisensory audiovisual (a₁v₁, **AV**) stimulus combination in which one visual stimulus is

129 presented together with one auditory stimulus (**Figure 1A**). In the EEG experiment, prior
130 to the audiovisual stimulation, participants performed an n-back task (0-back, 2-back).
131 In the current study, we only analyzed the a₀v₁ and a₁v₁ trials and only from the 0-back
132 condition. Further details of the experimental setup can be found in Michail et al. (2021),
133 which analyzed the memory-load effects on the perception of the a₂v₁ trials from the
134 same EEG dataset. The visual (flash) stimulus was a white disk subtending a visual
135 angle of 1.6° and was presented at 4.1° centrally below the fixation cross, for 13.3 ms
136 (EEG) or 16.7 ms (ECoG). The slight difference in visual presentation times is explained
137 by the different refresh rates of the displays used for the EEG and ECoG experiments.
138 The auditory (beep) stimulus was a 78 dB (SPL) 1000 Hz sine wave tone that was
139 presented for 7 ms. In AV trials, auditory and visual stimuli were presented
140 simultaneously.

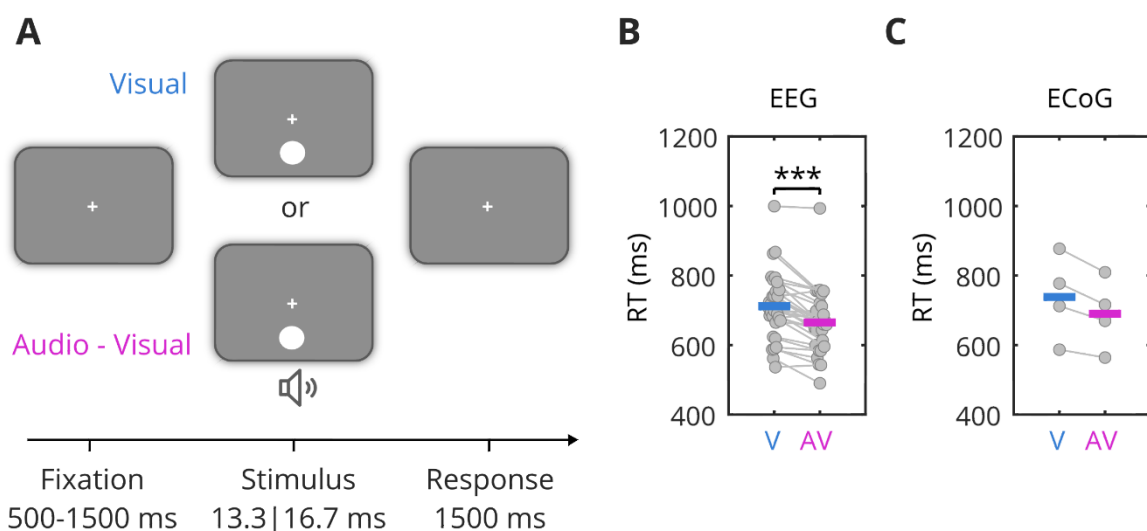
141
142 Stimulus presentation and recording of participants' responses were implemented using
143 the Psychophysics toolbox (Brainard, 1997; RRID:SCR_002881) for MATLAB (The
144 Mathworks, Natick, MA, USA). The EEG experiment was conducted in a dimly lit,
145 electrically shielded, noise-attenuating chamber. Visual stimuli were displayed on a 21-
146 inch CRT screen at a distance of 1.2 m with a 75 Hz refresh rate. The ECoG experiment
147 was conducted at the patient's bedside using a portable computer (HP Pavilion 17) with
148 a 60 Hz screen refresh rate. Auditory stimuli in both experiments were controlled by a
149 USB audio interface (UR22mkII, Steinberg) and delivered through in-ear headphones
150 (ER30, Etymotic Research).

151
152 Each trial started with a central fixation cross displayed for a variable duration of 500 to
153 800 ms (EEG) or 1000 to 1500 ms (ECoG). Then, one of the stimulus combinations was
154 presented. After the presentation of a stimulus, the fixation cross was displayed again

155 and participants had to indicate the number of perceived flashes by a button press (three
156 buttons: 0, 1 or 2). Following the button press or after 1500ms (if no button was pressed),
157 a new trial started. In the EEG experiment, prior to the main task described above,
158 participants performed a verbal visual n-back task (0- and 2-back, for details see Michail
159 et al., 2021). In the current study, we only used trials from the 0-back condition, in which
160 participants had to detect the target letter 'X', presented in 33% of all trials. The letter
161 detection task was not related to the V and AV stimuli and should, thus, not have
162 substantially affected the processing of these stimuli. Participants reported the number
163 of flashes with the right thumb using a handheld gamepad (Logitech Gamepad F310,
164 Logitech, Lausanne, Switzerland).

165

166 The EEG experiment included 12 blocks (6 blocks for each load level: 0-back and 2-
167 back), each block consisting of 74 trials. The order of blocks was randomized across
168 participants and the duration of experiment was approximately 80 minutes. The ECoG
169 experiment, with a duration of 60 minutes, consisted of 6 blocks, each including 139
170 trials (due to fatigue, the first participant completed only 4 blocks).



171 **Figure 1. Experimental setup and behavioral results.** A. Schematic illustration of the experimental
172 conditions. Participants were presented with a unisensory visual (V) or a bisensory audio-visual stimulus

173 (AV) and were asked to indicate the number of perceived visual stimuli. **B.** Participants in the EEG
174 experiment responded faster in the AV compared with the V condition. Horizontal bold lines denote the
175 mean. **C.** In the ECoG experiment, participants showed a speeding of responses in the AV condition,
176 similar to the EEG experiment. Within-subject response speed was faster for AV compared with V stimuli
177 in 3 out of 4 participants (significant or trend to significant difference). *** $p < 0.001$

178

179 **Behavioral data analysis**

180 Behavioral performance was assessed in terms of the percentage of correct responses
181 in the V and the AV condition and the RTs in trials with correct responses.

182

183 **Data acquisition and preprocessing**

184 High-density EEG was recorded using a 128-channel passive system (EasyCap,
185 Herrsching, Germany) at a sampling rate of 2500 Hz. Two electrodes, at the right lateral
186 canthi and below the right eye, recorded the horizontal and vertical electro-oculograms.
187 Preprocessing was performed with MNE-Python (Gramfort et al., 2014;
188 RRID:SCR_005972) and further data analysis with Fieldtrip (Oostenveld et al., 2011;
189 RRID:SCR_004849) and custom-made Matlab scripts (MathWorks, Natick, MA).

190

191 Offline, EEG data were filtered with a zero-phase bandpass finite impulse response
192 (FIR) filter between 1 Hz and 100 Hz using the window design method (“firwin” in SciPy
193 [<https://docs.scipy.org/doc/>]; Hanning window; 1 Hz lower transition bandwidth; 25 Hz
194 upper transition bandwidth; 3.3 s filter length). A band-stop notch FIR filter from 49 to 51
195 Hz (6.6 s filter length), was applied to remove line noise. In the next analysis step, data
196 were downsampled to 256 Hz and epoched from -1.5 to 1.5 s relative to the onset of the
197 stimuli. Trials with artefacts (eye blinks, noise, or muscle activity) were removed after
198 visual inspection. Data were then re-referenced to the average of all electrodes and
199 subjected to Independent Component Analysis (ICA) using the Extended-Infomax

200 algorithm (Lee et al., 1999). Components representing eye blinks, cardiac and muscle
201 activity were removed from the data. Next, noisy electrodes were rejected after visual
202 inspection on a trial-by-trial basis and interpolated using spherical spline interpolation
203 (Perrin et al., 1989). Finally, trials with signal exceeding $\pm 150 \mu\text{V}$ were excluded. On
204 average, across participants, 106.5 (SD 96) trials and 12.1 (SD 4.3) ICA components
205 were removed, and 11.1 (SD 3.6) electrodes were interpolated.

206
207 ECoG signals were recorded at a 2048 Hz sampling rate using a 128-channel REFA
208 system (TMSi International, Enschede, The Netherlands). Offline, ECoG data were
209 filtered using a zero-phase bandpass finite impulse response (FIR) filter between 1 Hz
210 and 200 Hz (high pass: order = 6765, -6 dB cutoff frequency = 0.5 Hz; low pass: order
211 = 137, -6 dB cutoff frequency = 225 Hz). A band-stop notch filter was applied at 50 Hz
212 (± 1) and its harmonics to filter out line noise. Data were subsequently downsampled to
213 600 Hz and epoched from -1 to 2.5 s relative to the onset of the stimulus. Electrodes
214 with epileptiform activity or excessive noise were excluded from the analysis. Moreover,
215 trials with an amplitude larger than five times the SD for more than a period of 25 ms
216 (Blenkmann et al., 2019) and trials with artefacts (large slow drifts or excessive noise)
217 identified after visual inspection were removed. Data were then re-referenced to the
218 common average. On average, across participants in the ECoG experiment, 11.4 % (SD
219 4.3) of the trials and 7.4 % (SD 5.8) of the electrodes were removed.

220
221 To determine the locations of the intracranial electrodes, the post-implantation CT was
222 co-registered with the preoperative MRI following the pipeline implemented in FieldTrip
223 for the integrated analysis of anatomical and ECoG data (Stolk et al., 2018).

224
225 **Time-frequency analysis**

226 Oscillatory power was computed by applying a Hanning taper to an adaptive time
227 window of 4 cycles for each frequency from 2 to 40 Hz, shifted from -1.5 to 1.5 s (EEG)
228 and from -1 to 2.5 s (ECoG), in steps of 10ms. Poststimulus power was baseline
229 corrected using the average power of the prestimulus window from -500 to -100 ms,
230 relative to stimulus onset.

231

232 **EEG source analysis**

233 Surface-level EEG data were projected into source space to investigate the cortical
234 sources of the correlation between spectral power and RTs, obtained from the sensor
235 level analysis. First, for each participant, the individual T1-weighted MRI (3T Magnetom
236 TIM Trio, Siemens, AG, Germany) was co-registered with the individually digitized EEG
237 electrode positions (Polhemus FastTrak) to a common coordinate system (Montreal
238 Neurological Institute, MNI). This was done by utilizing the digitized headshape
239 information and the fiducial locations (nasion, left and right preauricular points). The co-
240 registered MRI image was then segmented using the SPM12 algorithm and a realistic
241 three-shell (brain, skull, skin) boundary element volume conductor model (BEM) was
242 constructed (Oostendorp and van Oosterom, 1989). Next, the template MNI brain was
243 non-linearly warped onto each participant's anatomical data to obtain a three-
244 dimensional source model (volumetric grid) with a resolution of 10 mm, which was used
245 for the further analysis. To estimate the current density distribution the eLoreta algorithm
246 (Pascual-Marqui, 2007) was used with a lambda regularization parameter set to 1%. To
247 this end, the cross-spectral density (CSD) matrix was calculated using the Fast Fourier
248 Transform (FFT) method for the condition-pooled data. As mentioned in the Introduction,
249 in the current study, we were particularly interested on whether crossmodal RT
250 facilitation is associated with early crossmodal influences. Accordingly, the source
251 analysis focused on the early beta band component (80-200 ms, 13-25 Hz) of the

252 significant cluster obtained from the scalp level correlation analysis. Therefore, CSD
253 was calculated in the time window from 80 to 200 ms relative to stimulus onset. Center
254 frequency and spectral smoothing were defined to fit the frequency range of interest;
255 hence, a center frequency of 19 Hz and a smoothing of 6 Hz were used, resulting in a
256 13–25 Hz range. The current density estimate was normalized to the source estimate
257 for the baseline window (-0.5 to -0.1 s) as follows: $(Poststimulus - Baseline) /$
258 $(Poststimulus + Baseline)$.

259

260 **Statistical analysis**

261 For the EEG experiment, paired-samples *t*-tests were used to compare behavioral
262 performance, i.e., accuracy and RTs, between V and AV conditions. The corresponding
263 within-subject comparisons in the ECoG experiment were performed using independent-
264 samples *t*-tests.

265

266 To compare the EEG spectral power between V and AV conditions, a nonparametric
267 cluster-based permutation test was conducted (cluster-forming alpha = 0.05, dependent
268 *t*-test, iterations = 1000; Maris and Oostenveld, 2007). The test was applied in the time
269 window from 0 to 500 ms relative to stimulus onset, on frequencies from 2 to 40 Hz. The
270 observed test statistic was evaluated against the permutation distribution in order to test
271 the null hypothesis of no difference between conditions (two-tailed test, alpha = 0.025).

272

273 A nonparametric cluster-based permutation test was also applied to assess the
274 correlation between the AV minus V power difference at the sensor level and the RT
275 difference between the two conditions (cluster-forming alpha = 0.05, Spearman's rank
276 correlation, iterations = 1000). Accordingly, a similar approach was used for the
277 corresponding correlation analysis of the source space data (one-sided cluster-based

278 permutation test, cluster-forming alpha = 0.1, Spearman's rank correlation, iterations =
279 1000). As mentioned before, the source analysis aimed to further investigate the findings
280 of the sensor level analysis. Therefore, the direction of the one-tailed test was
281 determined by the sensor level results.

282
283 With regard to the analysis of the ECoG data, the difference in beta power (averaged
284 across the 13-25 Hz range) between V and AV conditions was assessed for each
285 electrode in the time window from 0 to 500 ms using a nonparametric cluster-based
286 permutation test (cluster-forming alpha = 0.05, independent samples *t*-test, iterations =
287 1000). Given that the non-symmetric arrangement of grid and strip electrodes prevents
288 the use of spatial clustering algorithms, a more restricted alpha threshold of $p = 0.01$
289 was applied.

290

291 **Results**

292

293 **Behavior**

294 Behavior was assessed in terms of how fast and how accurate participants responded
295 to V and AV stimuli. As depicted in **Figure 1B**, participants in the EEG experiment
296 responded faster in the AV compared with the V condition (mean \pm SD: 665 ± 92 ms vs.
297 712 ± 97 ms; paired samples *t*-test, $t_{(29)} = 6.7$, $p < 0.001$). Similarly, within-subject
298 comparisons for participants in the ECoG experiment revealed significantly faster or a
299 trend for faster responses in AV compared with the V condition in 3 out of 4 participants
300 (**Figure 1C**; independent samples *t*-test, participant #1: 670 ± 97 ms vs. 712 ± 98 ms,
301 $t_{(91)} = -2.1$, $p = 0.038$; #2: 716 ± 157 ms vs. 777 ± 193 ms, $t_{(150)} = -2.2$, $p = 0.033$; #3: 809
302 ± 182 ms vs. 877 ± 197 ms, $t_{(131)} = -2.1$, $p = 0.041$; #4: 564 ± 88 ms vs. 587 ± 87 ms,
303 $t_{(150)} = -1.6$, $p = 0.11$). Only participant #4 revealed similar performance between

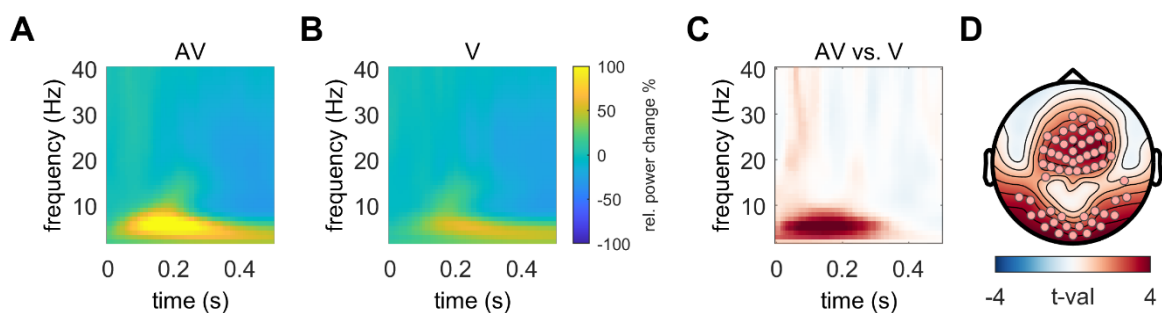
304 conditions ($p = 0.11$). As this participant responded much faster than the other three
305 participants, it is possible that the absence of a RT facilitation is due to a ceiling effect
306 in performance. In the EEG experiment, while responses were more accurate in AV than
307 V trials ($98.1 \pm 2.3\%$ vs. $92.0 \pm 8.9\%$, $t(29) = -3.9$, $p < 0.001$), participants showed in
308 general high accuracy ($>90\%$), suggesting that the task was easy to perform. Similarly,
309 responses in the ECoG experiment were also highly accurate (V: $92.7 \pm 5\%$, AV: $93 \pm$
310 6.9% ; individual accuracies: participant #1: V=90.4%, AV= 88.5%; #2: V=96.2%, AV=
311 100%; #3: V=86.8%, AV= 85.9%; #4: V=97.4%, AV= 97.4%). Taken together, behavioral
312 data from both EEG and ECoG experiments revealed that participants responded faster
313 when the visual stimulus was combined with a task-irrelevant auditory stimulus than
314 when the visual stimulus was presented alone.

315

316 **Audiovisual stimulation induces increased EEG theta power**

317 In the first step we analyzed the difference in EEG oscillatory power between the AV
318 and V condition in the window from 0 to 500 ms, on frequencies from 2 to 40 Hz, using
319 only correct trials. As illustrated in **Figure 2**, the nonparametric cluster-based
320 permutation test revealed stronger theta power increase in the AV compared with the V
321 condition, over medio-frontal and occipital electrodes in the time window from 0 to 400
322 ms relative to stimulus onset ($p = 0.003$).

323



324 **Figure 2. Oscillatory power difference between AV and V trials.** The cluster-based analysis of EEG
325 oscillatory power revealed higher theta power in AV compared with V trials in medio-frontal and occipital
326 electrodes. **A-B.** TFRs of oscillatory power modulation after AV and V stimulation, averaged across

327 electrodes with high contribution to the cluster (i.e., with a total number of significant time-frequency
328 samples at or above the mean). **C.** TFR of AV-V power difference (in t-values), averaged across
329 electrodes with high contribution to the cluster and masked based on the temporal and spectral extent of
330 the cluster. Higher values indicate stronger power for AV compared with the V condition. The color scale
331 refers only to unmasked t values. **D.** Topographic map showing the spatial distribution of the difference
332 in the cluster's time-frequency window. Electrodes with high contribution to the cluster are highlighted with
333 dots.

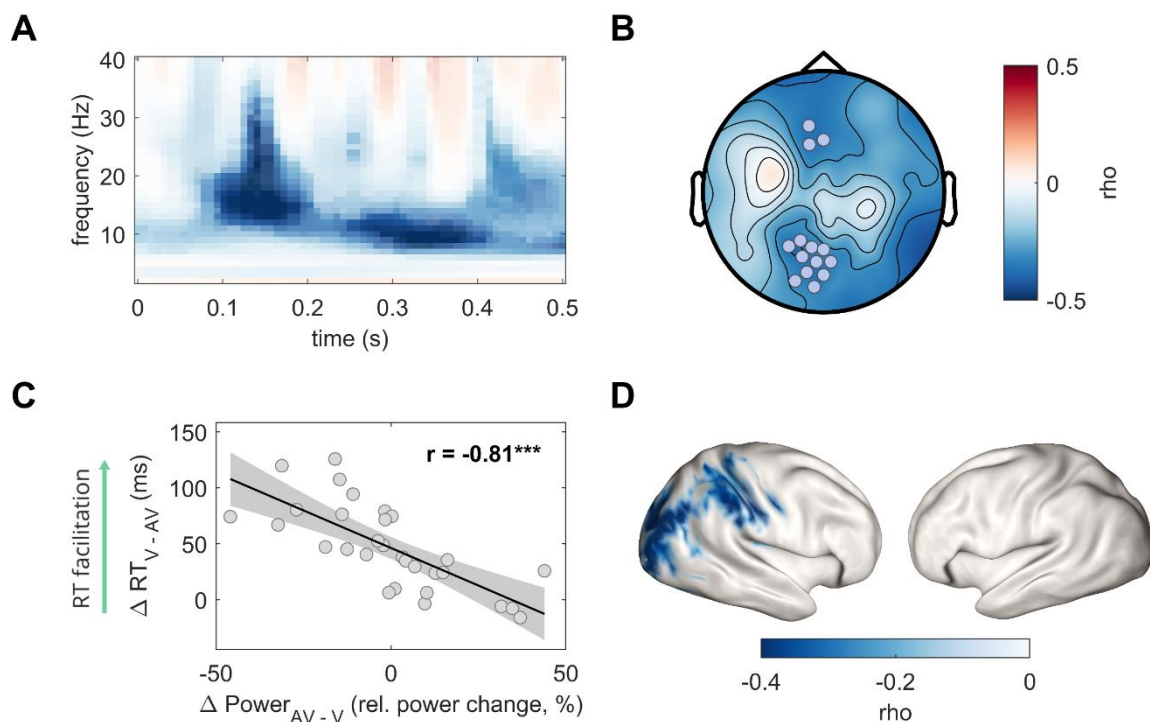
334

335 **Early beta power in association areas correlates with crossmodal facilitation of** 336 **response speed**

337 We next examined whether differences in EEG oscillatory power between the AV and
338 the V condition correlated with the crossmodal facilitation of RTs. (**Figure 1B**). For this
339 analysis only correct trials were used. A nonparametric cluster-based permutation test
340 revealed one significant cluster ($p = 0.001$) showing a negative correlation between the
341 RT difference (ΔRT_{V-AV}) and the power difference ($\Delta Power_{AV-V}$) over mainly parieto-
342 occipital and frontal scalp regions (**Figure 3A-B**). The cluster comprised two
343 components, one in the early beta band activity (strongest effect at 80-200 ms, 13-25
344 Hz) and a second one in the late alpha band activity (strongest effect at 250-400 ms, 8-
345 12Hz). To confirm the finding of the cluster-based analysis, a Spearman's rank
346 correlation was performed between the RT facilitation (V minus AV) and the AV minus
347 V power difference in the cluster (**Figure 3C**; $\rho = -0.81$, $p < 0.001$). A comparison of
348 the power in the cluster between the V and AV conditions revealed no significant
349 difference between the two conditions. As mentioned in the *Introduction*, a central aim
350 of the current study was to identify potential crossmodal effects at early processing
351 stages. Therefore, the corresponding correlation analysis for the source activity focused
352 on the early beta band activity (80-200 ms, 13-25 Hz). This analysis revealed a
353 significant negative correlation of the AV minus V beta power difference in areas of the

354 right inferior parietal and extrastriate occipital cortex with the crossmodal RT facilitation
355 (nonparametric cluster-based permutation test, $p = 0.001$).

356
357 Taken together, our analysis revealed that the lower the early, parieto-occipital beta
358 power in the AV compared with the V condition the faster participants responded in the
359 AV vs. V condition. Moreover, the source localization of this correlation suggests the
360 involvement of multisensory association areas and secondary visual cortex during the
361 crossmodal RT facilitation.



362 **Figure 3. Correlation between AV minus V power difference and the crossmodal RT facilitation.**

363 The cluster-based correlation analysis revealed that crossmodal RT facilitation was associated with
364 reduced beta power at 80-200 ms and reduced alpha power at 250-400 ms in mainly parieto-occipital
365 electrodes, with the earlier beta effect being localized in inferior parietal and extrastriate occipital areas.

366 **A.** TFR of the correlation (in rho values) between the AV minus V power difference and the V minus AV
367 RT difference, averaged across electrodes with the highest contribution to the cluster (i.e., with a total
368 number of significant time-frequency samples at or above the 75th percentile) and masked based on the
369 temporal and spectral extent of the cluster. Lower values (blue) indicate that crossmodal RT facilitation
370 correlates with smaller AV minus V power difference. The color scale refers only to unmasked rho values.

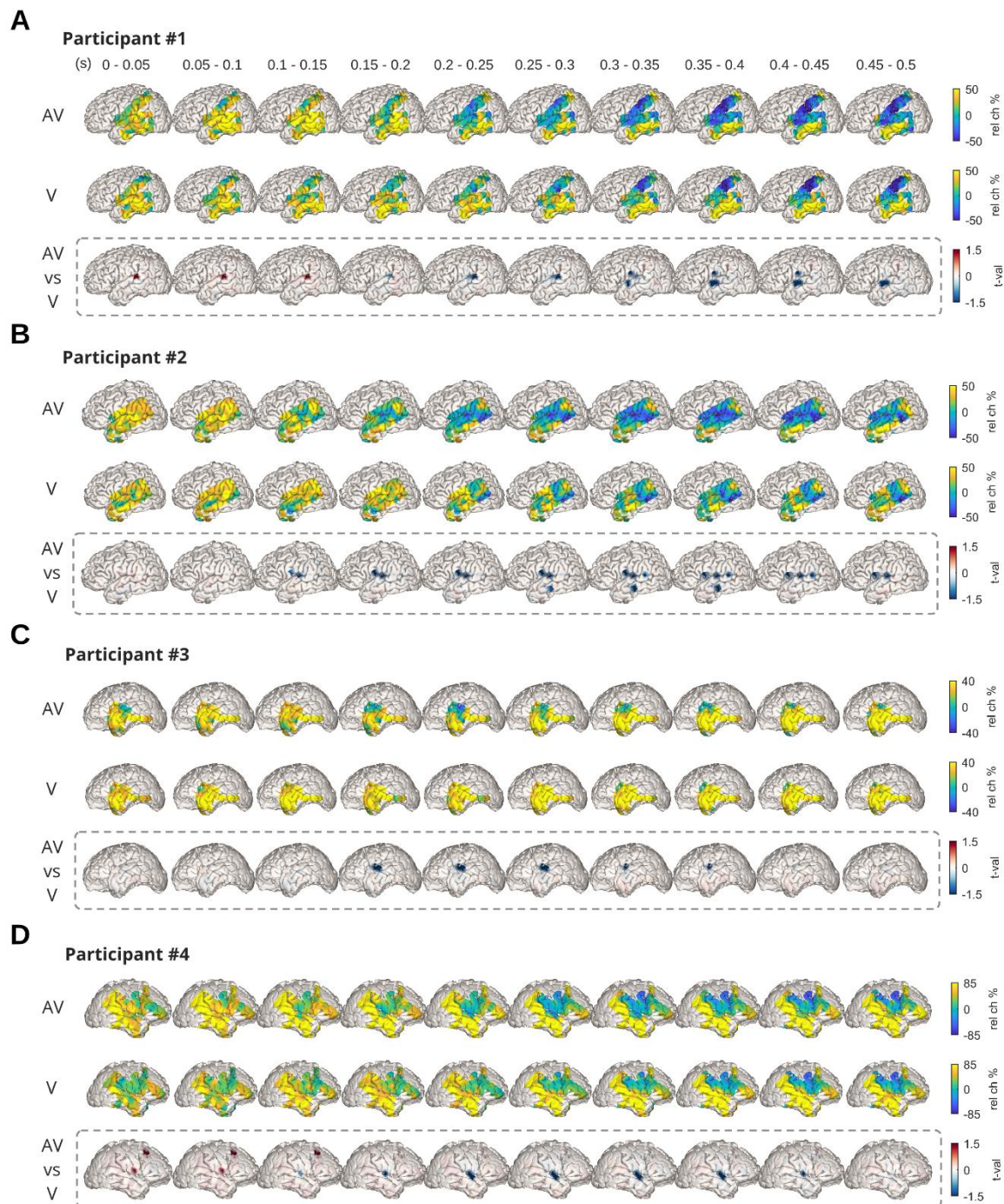
371 **B.** Topographic map showing the distribution of the correlation between AV minus V power difference and
372 the crossmodal RT facilitation. Electrodes with the highest contribution to the cluster are highlighted with
373 dots. **C.** Scatterplot depicting the correlation between the individual power difference (A minus V) in the
374 cluster and the crossmodal RT facilitation (i.e., V minus AV). The lower the power in the cluster for the AV
375 compared with the V condition the larger the crossmodal RT facilitation. Black lines represent the best-
376 fitting linear regression and shaded areas the 95% confidence interval. **D.** Correlation in source space
377 between the early beta band power difference (AV minus V, 80-200 ms, 13-25 Hz) and the crossmodal
378 RT facilitation. Lower AV vs. V beta power in inferior parietal and extrastriate visual areas correlated with
379 the crossmodal RT facilitation.; *** $p < 0.001$

380

381 **ECoG beta power in the superior temporal gyrus is lower in audiovisual compared** 382 **with visual-only trials**

383 To further examine the role of beta power during crossmodal processing, we compared
384 beta power modulations between the unisensory V and bisensory AV conditions in four
385 participants implanted with intracranial electrodes covering mainly the temporal cortex
386 (**Figure 4**). As reported above, these participants displayed shorter RTs for the AV
387 compared with the V condition (**Figure 1C**). Our primary interest in this study, was to
388 investigate early crossmodal influences on neural oscillations. Therefore, based on the
389 outcome of the EEG data analysis – which linked early beta power modulations with
390 crossmodal RT facilitation – the ECoG data analysis focused on the time course of the
391 beta band power (13-25 Hz). This analysis revealed that, consistently for all four
392 participants, beta power in the superior temporal gyrus (STG) starting at approximately
393 130 to 150 ms poststimulus was significantly lower in the AV compared with the V
394 condition (nonparametric cluster-based permutation test, $p < 0.01$). Interestingly, the
395 reverse pattern was observed for very early beta power (< 100 ms) in few electrodes in
396 participant #1 (STG) and participant #4 (rolandic operculum, middle frontal gyrus). In
397 these electrodes, beta power in the first 100 ms after stimulus onset was significantly

398 higher in AV compared with V trials. **Table 1** provides an overview of the statistical
399 results and the MNI coordinates of the electrodes at which significant effects were
400 observed. These results provide further evidence that beta band power modulations in
401 multisensory association areas, and especially in STG, reflect early crossmodal
402 influences that might play a critical role in crossmodal RT facilitation.



403 **Figure 4. Intracranial (ECoG) beta band power in response to AV and V stimuli.** The comparison of
404 ECoG beta band power between the AV and the V condition showed that, consistent across participants,

405 beta power in STG starting at approximately 150 ms after stimulus onset was significantly lower in AV
 406 compared with the V condition. **A-D**. For each participant, the first two rows display the beta band (13-25
 407 Hz) power modulation after AV and V stimulation in the time window from 0 to 500 ms after stimulus onset.
 408 The third row (highlighted with a dotted line) shows the beta band power difference (in *t*-values) between
 409 AV and V conditions. Larger values (red) indicate stronger power for AV compared with the V condition.
 410

Table 1. Comparison of beta power between V and AV trials in ECoG experiment

Elec	MNI Coordinates			Region (AAL atlas)	Statistical results				
					AV > V		AV < V		
						<i>interval (s)</i>	<i>p_{cluster}</i>	<i>interval (s)</i>	<i>p_{cluster}</i>
Participant #1									
A28	-66.4698	-32.2866	14.2284	Superior temporal gyrus, L	0.01 - 0.12	.003		0.19 - 0.28	.005
A29	-66.1779	-21.6054	13.3358	Superior temporal gyrus, L				0.24 - 0.34	.006
B16	-63.8651	-12.4889	19.5746	Postcentral gyrus, L				0.31 - 0.44	.002
A23	-63.7925	-3.8424	-0.7619	Superior temporal gyrus, L				0.34 - 0.49	.002
A22	-66.4068	-13.4439	0.1332	Middle temporal gyrus, L				0.38 - 0.50	.007
Participant #2									
A21	-68.0743	-18.6511	12.6049	Superior temporal gyrus, L				0.13 - 0.50	.001
A30	-64.8222	-2.9299	16.5722	Postcentral gyrus, L				0.15 - 0.34	.001
A06	-69.7984	-19.5751	-14.4308	Middle temporal gyrus, L				0.30 - 0.39	.005
A11	-68.2180	-43.3035	14.4621	Superior temporal gyrus, L				0.35 - 0.43	.007
A31	-60.2779	6.0567	10.7324	Inferior frontal gyrus, opercular, L				0.39 - 0.49	.004
Participant #3									
A06	-68.2460	-9.0777	-4.1051	Middle temporal gyrus, L				0.16 - 0.29	.001
A11	-64.9019	-0.7296	1.0793	Superior temporal gyrus, L				0.17 - 0.37	.002
Participant #4									
A24	64.2172	4.7504	8.4491	Rolandic operculum, R	0.00 - 0.09	.007			
E03	44.2111	29.7326	46.4387	Middle frontal gyrus, R	0.02 - 0.12	.008			
A23	66.3881	-3.1604	2.5210	Superior temporal gyrus, R				0.15 - 0.41	.001
A27	62.8264	3.1071	-7.3572	Superior temporal pole, R				0.22 - 0.37	.001

411

412

413

414 **Discussion**

415 In this study, we analyzed EEG and ECoG data to elucidate the neural correlates of the
416 crossmodal RT facilitation, as manifested in the speeding of behavioral responses to
417 visual stimuli by the addition of task-irrelevant auditory information. We showed that
418 reduced beta power in the AV compared with V trials correlated with individual
419 crossmodal RT gains. This effect occurred around 80-200 ms poststimulus in parieto-
420 occipital electrodes and was localized in secondary visual and multisensory association
421 areas. Moreover, the ECoG data analysis showed that beta power in the STG, which is
422 a key multisensory association area, is reduced in AV compared with V trials, starting
423 approximately 150 ms after stimulus onset. These findings provide evidence that beta
424 band power modulations in multisensory association and secondary visual cortex during
425 early visual sensory processing reflect the crossmodal facilitation of response speed.

426
427 Despite evidence of crossmodal influences occurring during both early and late
428 multisensory processing and in both primary sensory and higher-order cortical areas
429 (Macaluso and Driver, 2005; Koelewijn et al., 2010; Talsma et al., 2010; Keil and
430 Senkowski, 2018), it is not well understood how such interactions enable the
431 multisensory facilitation of performance. A central question regards the processing stage
432 and the level of cortical hierarchy at which information from one modality influences
433 another modality, in particular when such multisensory influences facilitate performance
434 (Bizley et al., 2016).

435
436 Our finding that crossmodal RT facilitation was linked with oscillatory power modulations
437 at 80-200 ms poststimulus suggests that the auditory signal influenced early visual
438 sensory processing to enhance performance. This result is consistent with a large body
439 of primate and human electrophysiological studies demonstrating multisensory

440 interactions at early processing stages (Giard and Peronnet, 1999; Molholm et al., 2002;
441 Schroeder and Foxe, 2005; Talsma and Woldorff, 2005; Lakatos et al., 2007; Kayser et
442 al., 2010; Mercier et al., 2013). Moreover, our finding is in line with EEG studies providing
443 direct evidence of early crossmodal responses underlying multisensory behavior
444 facilitation in tasks using simple audiovisual stimuli (Thorne et al., 2011; Van der Burg
445 et al., 2011; Starke et al., 2020). On the contrary, other studies using more complex
446 stimuli have shown that sound-induced improvements of visual motion and visual object
447 categorization were associated with late single-trial EEG activity starting at 300 ms
448 (Kayser et al., 2017; Franzen et al., 2020). This divergence in the latency of
449 performance-relevant crossmodal influences is consistent with evidence of multisensory
450 integration taking place during both sensory encoding and decision formation (Mercier
451 and Cappe, 2020) and is likely attributed to stimulus complexity, in accordance with the
452 adaptive engagement of integrative mechanisms depending on task-specific
453 characteristics (van Atteveldt et al., 2014; Bizley et al., 2016). In this framework, our
454 data argue that under conditions of low stimulus complexity, multisensory RT facilitation
455 is linked with crossmodal influences at early processing stages.

456
457 Critically, the crossmodal RT facilitation in our study was associated with power
458 modulations in the beta band (13-25 Hz). The correlation between crossmodal beta
459 power modulation and RT facilitation was observed in parieto-occipital electrodes and
460 was localized in inferior parietal and extrastriate occipital regions. We propose that the
461 performance-relevant beta power suppression in the audiovisual compared with the
462 visual condition reflects the enhancement of early visual processing through top-down
463 attentional control originating from multisensory association and secondary visual
464 cortex. This proposal is consistent with growing evidence on the role of beta oscillations
465 in conveying feedback influences on low-level visual areas (Buschman and Miller, 2007;

466 Kerkoerle et al., 2014; Bastos et al., 2015; Michalareas et al., 2016; Richter et al., 2017;
467 Limanowski et al., 2020). Moreover, evidence of feedback influences in the alpha-beta
468 band modulating feedforward gamma band processing (Spaak et al., 2012; Richter et
469 al., 2017) suggests that feedback signals in the low-frequency range (i.e., in the alpha-
470 beta range), originating from association areas can directly modulate the feedforward
471 stream of information during early sensory processing (Bressler and Richter, 2015). Our
472 proposal is further supported by research showing that the suppression of low-frequency
473 activity is associated with more efficient sensory processing of task-relevant signals
474 (Klimesch et al., 2007; Jensen and Mazaheri, 2010), possibly by enhancing the
475 feedforward communication through gamma band coherence (Hahn et al., 2019). In
476 multisensory settings, previous studies provided evidence implicating beta power in the
477 audiovisual redundant target effect (Senkowski et al., 2006), the integration of
478 incongruent or noisy audiovisual speech stimuli (Schepers et al., 2013; Roa Romero et
479 al., 2015), crossmodal influence on pain (Senkowski et al., 2011; Mancini et al., 2013),
480 and the impact of working memory load on audiovisual illusory perception (Michail et al.,
481 2021). Moreover, previous research demonstrated the involvement of beta band
482 functional connectivity between primary and higher-order association areas in
483 multisensory perception (Kayser and Logothetis, 2009; Hipp et al., 2011; Keil et al.,
484 2014). Interestingly, a crossmodal (AV minus V) theta power enhancement over medio-
485 frontal and occipital regions was not related to performance enhancement, suggesting
486 that crossmodal theta power modulations might not be directly relevant for behavior. In
487 this context, we argue that the functionally relevant beta band suppression in secondary
488 visual and multisensory association areas – driven by the task-irrelevant auditory
489 stimulus – enhanced early sensory representations of the visual stimulus through top-
490 down attentional control of feedforward information processing.

491

492 Additionally, the analysis of the ECoG data revealed that beta power was reduced in the
493 STG in the AV compared with the V condition. Previous work has established the critical
494 role of the STG in multisensory perception, acting as a convergence hub for inputs from
495 multiple modalities (Calvert et al., 2000; Beauchamp et al., 2004; Barraclough et al.,
496 2005; Balz et al., 2016; Ozker et al., 2017; Karas et al., 2019; Mégevand et al., 2020).
497 Moreover, previous studies using illusory audiovisual paradigms demonstrated that beta
498 band power suppression was associated with audiovisual mismatch evaluation and top-
499 down influences on audiovisual integration, induced by working memory load (Roa
500 Romero et al., 2015; Michail et al., 2021). In accordance with these studies, the beta
501 band suppression in the STG might reflect an auditory-driven feedback signal to improve
502 visual processing through selective attention. This notion is consistent with the temporal
503 and spatial profile of the observed tight relationship between beta oscillations in the EEG
504 data and the crossmodal RT facilitation. It also in line with neuroimaging and
505 electrophysiological evidence showing anatomical and functional connections in the
506 beta band between STG and primary sensory areas (Noesselt et al., 2007, 2010; Cappe
507 et al., 2009; Kayser and Logothetis, 2009; Keil et al., 2014). Therefore, this finding,
508 together with the sources of the correlation between EEG beta power and RT facilitation,
509 suggest an important role of multisensory association areas during behaviorally relevant
510 early crossmodal processing.

511
512 Thus far, only few studies have investigated the oscillatory signatures of crossmodal RT
513 facilitation using similar audiovisual stimuli as the current study (Senkowski et al., 2006;
514 Mercier et al., 2015). Contrary to present findings, one previous study found that the
515 audiovisual RT facilitation was associated with increased evoked beta power in left
516 frontal and right occipital electrodes (Senkowski et al., 2006). This inconsistent finding
517 might be explained by differences in the task instructions. In the current study

518 participants had to report on features of the visual stimulus, whereas in Senkowski et al.
519 (2006) participants made speeded responses upon stimulus detection independent of
520 modality. This resulted in markedly faster RTs in Senkowski et al. (2006) compared with
521 the current study (mean RTs to AV trials: 255 ms vs. 665 ms, respectively). Thus, the
522 beta modulations in that previous study were possibly related to motor processes,
523 whereas, in the present study, there is an additional perceptual aspect. Using a similar
524 speeded detection task, an ECoG study has linked crossmodal RT facilitation with local
525 phase alignment and phase synchronization between auditory and motor cortex in the
526 delta band (Mercier et al., 2015). The use of a speeded detection task in these studies
527 makes it difficult to disentangle the oscillatory activities associated with audiovisual
528 interactions in sensory and non-sensory stages of information processing. Further
529 investigations are required to differentiate the contributions of beta power and functional
530 connectivity at the level of sensory processing, decision-making and motor response.

531
532 One limitation of our study is the small sample size in the ECoG experiment, which
533 prevented us from performing similar analyses as in the EEG experiment. In addition to
534 that, the heterogeneity between participants in the cortical grid coverage, further
535 constrained the ability to perform analyses across participants to obtain statistically
536 robust results at the group level. Thus, future ECoG studies, recruiting larger participant
537 cohorts and possibly with a more diverse cortical grid coverage could provide insights
538 into the role of other regions in crossmodal performance enhancement.

539
540 Altogether, our data suggest that beta power in multisensory association areas is related
541 to the crossmodal facilitation of response speed. This beta power modulation
542 presumably reflects the earliest stage of behaviorally relevant audiovisual feedback
543 processing in higher multisensory areas, starting around 80 ms after stimulus

544 presentation. Thus, the present findings highlight the important role of beta oscillations
545 in mediating behaviorally relevant crossmodal influences between the auditory and
546 visual modalities.

547

548 **References**

549 Balz J, Keil J, Roa Romero Y, Mекle R, Schubert F, Aydin S, Ittermann B, Gallinat J,
550 Senkowski D (2016) GABA concentration in superior temporal sulcus predicts
551 gamma power and perception in the sound-induced flash illusion. *NeuroImage*
552 125:724–730.

553 Barraclough NE, Xiao D, Baker CI, Oram MW, Perrett DI (2005) Integration of Visual
554 and Auditory Information by Superior Temporal Sulcus Neurons Responsive to
555 the Sight of Actions. *Journal of Cognitive Neuroscience* 17:377–391.

556 Bastos AM, Vezoli J, Bosman CA, Schoffelen JM, Oostenveld R, Dowdall JR, De Weerd
557 P, Kennedy H, Fries P (2015) Visual Areas Exert Feedforward and Feedback
558 Influences through Distinct Frequency Channels. *Neuron* 85:390–401.

559 Bauer AKR, Debener S, Nobre AC (2020) Synchronisation of Neural Oscillations and
560 Cross-modal Influences. *Trends Cogn Sci* 24:481–495.

561 Beauchamp MS, Lee KE, Argall BD, Martin A (2004) Integration of Auditory and Visual
562 Information about Objects in Superior Temporal Sulcus. *Neuron* 41:809–823.

563 Bizley JK, Jones GP, Town SM (2016) Where are multisensory signals combined for
564 perceptual decision-making? *Current Opinion in Neurobiology* 40:31–37.

565 Blenkmann AO, Collavini S, Lubell J, Llorens A, Funderud I, Ivanovic J, Larsson PG,
566 Meling TR, Bekinschtein T, Kochen S, Endestad T, Knight RT, Solbakk AK (2019)

- 567 Auditory deviance detection in the human insula: An intracranial EEG study.
568 Cortex 121:189–200.
- 569 Brainard DH (1997) The Psychophysics Toolbox. *Spat Vis* 10:433–436.
- 570 Bressler SL, Richter CG (2015) Interareal oscillatory synchronization in top-down
571 neocortical processing. *Current Opinion in Neurobiology* 31:62–66.
- 572 Buschman TJ, Miller EK (2007) Top-Down Versus Bottom-Up Control of Attention in the
573 Prefrontal and Posterior Parietal Cortices. *Science* 315:1860–1862.
- 574 Calvert GA, Campbell R, Brammer MJ (2000) Evidence from functional magnetic
575 resonance imaging of crossmodal binding in the human heteromodal cortex.
576 *Current Biology* 10:649–657.
- 577 Cappe C, Rouiller EM, Barone P (2009) Multisensory anatomical pathways. *Hearing*
578 *Research* 258:28–36.
- 579 Diederich A, Colonius H (2004) Bimodal and trimodal multisensory enhancement:
580 Effects of stimulus onset and intensity on reaction time. *Perception &*
581 *Psychophysics* 66:1388–1404.
- 582 Fort A, Delpuech C, Pernier J, Giard MH (2002) Dynamics of Cortico-subcortical Cross-
583 modal Operations Involved in Audio-visual Object Detection in Humans. *Cerebral*
584 *Cortex* 12:1031–1039.
- 585 Franzen L, Delis I, De Sousa G, Kayser C, Philiastides MG (2020) Auditory information
586 enhances post-sensory visual evidence during rapid multisensory decision-
587 making. *Nature Communications* 11:5440.

- 588 Giard MH, Peronnet F (1999) Auditory-Visual Integration during Multimodal Object
589 Recognition in Humans: A Behavioral and Electrophysiological Study. *Journal of*
590 *Cognitive Neuroscience* 11:473–490.
- 591 Gondan M, Niederhaus B, Rösler F, Röder B (2005) Multisensory processing in the
592 redundant-target effect: A behavioral and event-related potential study.
593 *Perception & Psychophysics* 67:713–726.
- 594 Gramfort A, Luessi M, Larson E, Engemann DA, Strohmeier D, Brodbeck C, Parkkonen
595 L, Hämäläinen MS (2014) MNE software for processing MEG and EEG data.
596 *NeuroImage* 86:446–460.
- 597 Hahn G, Ponce-Alvarez A, Deco G, Aertsen A, Kumar A (2019) Portraits of
598 communication in neuronal networks. *Nature Reviews Neuroscience* 20:117–
599 127.
- 600 Hershenson M (1962) Reaction time as a measure of intersensory facilitation. *Journal*
601 *of Experimental Psychology* 63:289–293.
- 602 Hipp JF, Engel AK, Siegel M (2011) Oscillatory Synchronization in Large-Scale Cortical
603 Networks Predicts Perception. *Neuron* 69:387–396.
- 604 Jensen O, Mazaheri A (2010) Shaping functional architecture by oscillatory alpha
605 activity: gating by inhibition. *Front Hum Neurosci* 4:186.
- 606 Karas PJ, Magnotti JF, Metzger BA, Zhu LL, Smith KB, Yoshor D, Beauchamp MS
607 (2019) The visual speech head start improves perception and reduces superior
608 temporal cortex responses to auditory speech Pasternak T, King AJ, Mahon B,
609 eds. *eLife* 8:e48116.

- 610 Kayser C, Logothetis NK (2009) Directed Interactions Between Auditory and Superior
611 Temporal Cortices and their Role in Sensory Integration. *Front Integr Neurosci*
612 3:7.
- 613 Kayser C, Logothetis NK, Panzeri S (2010) Visual Enhancement of the Information
614 Representation in Auditory Cortex. *Current Biology* 20:19–24.
- 615 Kayser SJ, Philiastides MG, Kayser C (2017) Sounds facilitate visual motion
616 discrimination via the enhancement of late occipital visual representations.
617 *NeuroImage* 148:31–41.
- 618 Keil J, Müller N, Hartmann T, Weisz N (2014) Prestimulus Beta Power and Phase
619 Synchrony Influence the Sound-Induced Flash Illusion. *Cereb Cortex* 24:1278–
620 1288.
- 621 Keil J, Senkowski D (2018) Neural Oscillations Orchestrate Multisensory Processing.
622 *The Neuroscientist* 24:609–626.
- 623 Kerkoerle T van, Self MW, Dagnino B, Gariel-Mathis MA, Poort J, Tooten C van der,
624 Roelfsema PR (2014) Alpha and gamma oscillations characterize feedback and
625 feedforward processing in monkey visual cortex. *PNAS* 111:14332–14341.
- 626 Klimesch W, Sauseng P, Hanslmayr S (2007) EEG alpha oscillations: the inhibition-
627 timing hypothesis. *Brain Res Rev* 53:63–88.
- 628 Koelewijn T, Bronkhorst A, Theeuwes J (2010) Attention and the multiple stages of
629 multisensory integration: A review of audiovisual studies. *Acta Psychologica*
630 134:372–384.

- 631 Lakatos P, Chen C-M, O'Connell MN, Mills A, Schroeder CE (2007) Neuronal
632 Oscillations and Multisensory Interaction in Primary Auditory Cortex. *Neuron*
633 53:279–292.
- 634 Lee TW, Girolami M, Sejnowski TJ (1999) Independent Component Analysis Using an
635 Extended Infomax Algorithm for Mixed Subgaussian and Supergaussian
636 Sources. *Neural Computation* 11:417–441.
- 637 Limanowski J, Litvak V, Friston K (2020) Cortical beta oscillations reflect the contextual
638 gating of visual action feedback. *NeuroImage* 222:117267.
- 639 Lippert M, Logothetis NK, Kayser C (2007) Improvement of visual contrast detection by
640 a simultaneous sound. *Brain Research* 1173:102–109.
- 641 Macaluso E, Driver J (2005) Multisensory spatial interactions: a window onto functional
642 integration in the human brain. *Trends in Neurosciences* 28:264–271.
- 643 Mancini F, Longo MR, Canzoneri E, Vallar G, Haggard P (2013) Changes in cortical
644 oscillations linked to multisensory modulation of nociception. *European Journal*
645 *of Neuroscience* 37:768–776.
- 646 Maris E, Oostenveld R (2007) Nonparametric statistical testing of EEG- and MEG-data.
647 *Journal of Neuroscience Methods* 164:177–190.
- 648 Mégevand P, Mercier MR, Groppe DM, Zion Golumbic E, Mesgarani N, Beauchamp
649 MS, Schroeder CE, Mehta AD (2020) Crossmodal Phase Reset and Evoked
650 Responses Provide Complementary Mechanisms for the Influence of Visual
651 Speech in Auditory Cortex. *J Neurosci* 40:8530–8542.

- 652 Mercier MR, Cappe C (2020) The interplay between multisensory integration and
653 perceptual decision making. *NeuroImage* 222:116970.
- 654 Mercier MR, Foxe JJ, Fiebelkorn IC, Butler JS, Schwartz TH, Molholm S (2013)
655 Auditory-driven phase reset in visual cortex: Human electrocorticography reveals
656 mechanisms of early multisensory integration. *Neuroimage* 79:19–29.
- 657 Mercier MR, Molholm S, Fiebelkorn IC, Butler JS, Schwartz TH, Foxe JJ (2015) Neuro-
658 Oscillatory Phase Alignment Drives Speeded Multisensory Response Times: An
659 Electro-Corticographic Investigation. *The Journal of Neuroscience* 35:8546–
660 8557.
- 661 Michail G, Senkowski D, Niedeggen M, Keil J (2021) Memory Load Alters Perception-
662 Related Neural Oscillations during Multisensory Integration. *J Neurosci* 41:1505–
663 1515.
- 664 Michalareas G, Vezoli J, van Pelt S, Schoffelen JM, Kennedy H, Fries P (2016) Alpha-
665 Beta and Gamma Rhythms Subserve Feedback and Feedforward Influences
666 among Human Visual Cortical Areas. *Neuron* 89:384–397.
- 667 Molholm S, Ritter W, Javitt DC, Foxe JJ (2004) Multisensory Visual–Auditory Object
668 Recognition in Humans: a High-density Electrical Mapping Study. *Cerebral*
669 *Cortex* 14:452–465.
- 670 Molholm S, Ritter W, Murray MM, Javitt DC, Schroeder CE, Foxe JJ (2002) Multisensory
671 auditory–visual interactions during early sensory processing in humans: a high-
672 density electrical mapping study. *Cognitive Brain Research* 14:115–128.
- 673 Noesselt T, Rieger JW, Schoenfeld MA, Kanowski M, Hinrichs H, Heinze HJ, Driver J
674 (2007) Audiovisual Temporal Correspondence Modulates Human Multisensory

- 675 Superior Temporal Sulcus Plus Primary Sensory Cortices. *J Neurosci* 27:11431–
676 11441.
- 677 Noesselt T, Tyll S, Boehler CN, Budinger E, Heinze H-J, Driver J (2010) Sound-Induced
678 Enhancement of Low-Intensity Vision: Multisensory Influences on Human
679 Sensory-Specific Cortices and Thalamic Bodies Relate to Perceptual
680 Enhancement of Visual Detection Sensitivity. *J Neurosci* 30:13609–13623.
- 681 Oostendorp TF, van Oosterom A (1989) Source parameter estimation in
682 inhomogeneous volume conductors of arbitrary shape. *IEEE Transactions on*
683 *Biomedical Engineering* 36:382–391.
- 684 Oostenveld R, Fries P, Maris E, Schoffelen JM (2011) FieldTrip: Open source software
685 for advanced analysis of MEG, EEG, and invasive electrophysiological data.
686 *Comput Intell Neurosci* 2011:156869.
- 687 Ozker M, Schepers IM, Magnotti JF, Yoshor D, Beauchamp MS (2017) A Double
688 Dissociation between Anterior and Posterior Superior Temporal Gyrus for
689 Processing Audiovisual Speech Demonstrated by Electrocorticography. *Journal*
690 *of Cognitive Neuroscience* 29:1044–1060.
- 691 Pascual-Marqui RD (2007) Discrete, 3D distributed, linear imaging methods of electric
692 neuronal activity. Part 1: exact, zero error localization. arXiv:07103341 [math-ph,
693 physics:physics, q-bio] Available at: <http://arxiv.org/abs/0710.3341>.
- 694 Perrin F, Pernier J, Bertrand O, Echallier JF (1989) Spherical splines for scalp potential
695 and current density mapping. *Electroencephalography and Clinical*
696 *Neurophysiology* 72:184–187.

- 697 Richter CG, Thompson WH, Bosman CA, Fries P (2017) Top-Down Beta Enhances
698 Bottom-Up Gamma. *J Neurosci* 37:6698–6711.
- 699 Roa Romero Y, Senkowski D, Keil J (2015) Early and late beta-band power reflect
700 audiovisual perception in the McGurk illusion. *Journal of Neurophysiology*
701 113:2342–2350.
- 702 Schepers IM, Schneider TR, Hipp JF, Engel AK, Senkowski D (2013) Noise alters beta-
703 band activity in superior temporal cortex during audiovisual speech processing.
704 *NeuroImage* 70:101–112.
- 705 Schroeder CE, Foxe J (2005) Multisensory contributions to low-level, ‘unisensory’
706 processing. *Current Opinion in Neurobiology* 15:454–458.
- 707 Senkowski D, Kautz J, Hauck M, Zimmermann R, Engel AK (2011) Emotional Facial
708 Expressions Modulate Pain-Induced Beta and Gamma Oscillations in
709 Sensorimotor Cortex. *J Neurosci* 31:14542–14550.
- 710 Senkowski D, Molholm S, Gomez-Ramirez M, Foxe JJ (2006) Oscillatory Beta Activity
711 Predicts Response Speed during a Multisensory Audiovisual Reaction Time
712 Task: A High-Density Electrical Mapping Study. *Cereb Cortex* 16:1556–1565.
- 713 Spaak E, Bonnefond M, Maier A, Leopold DA, Jensen O (2012) Layer-Specific
714 Entrainment of Gamma-Band Neural Activity by the Alpha Rhythm in Monkey
715 Visual Cortex. *Current Biology* 22:2313–2318.
- 716 Spence C, Driver J (2004) *Crossmodal Space and Crossmodal Attention*. Oxford
717 University Press.

- 718 Starke J, Ball F, Heinze HJ, Noesselt T (2020) The spatio-temporal profile of
719 multisensory integration. *European Journal of Neuroscience* 51:1210–1223.
- 720 Stolk A, Griffin S, Meij R van der, Dewar C, Saez I, Lin JJ, Piantoni G, Schoffelen J-M,
721 Knight RT, Oostenveld R (2018) Integrated analysis of anatomical and
722 electrophysiological human intracranial data. *Nat Protoc* 13:1699–1723.
- 723 Talsma D, Senkowski D, Soto-Faraco S, Woldorff MG (2010) The multifaceted interplay
724 between attention and multisensory integration. *Trends in Cognitive Sciences*
725 14:400–410.
- 726 Talsma D, Woldorff MG (2005) Selective attention and multisensory integration: multiple
727 phases of effects on the evoked brain activity. *J Cogn Neurosci* 17:1098–1114.
- 728 Thorne JD, Vos MD, Viola FC, Debener S (2011) Cross-Modal Phase Reset Predicts
729 Auditory Task Performance in Humans. *J Neurosci* 31:3853–3861.
- 730 Van der Burg E, Talsma D, Olivers CNL, Hickey C, Theeuwes J (2011) Early
731 multisensory interactions affect the competition among multiple visual objects.
732 *NeuroImage* 55:1208–1218.
- 733 van Atteveldt N, Murray MM, Thut G, Schroeder CE (2014) Multisensory Integration:
734 Flexible Use of General Operations. *Neuron* 81:1240–1253.
- 735
- 736
- 737
- 738